

# RSC Advances



This is an *Accepted Manuscript*, which has been through the Royal Society of Chemistry peer review process and has been accepted for publication.

*Accepted Manuscripts* are published online shortly after acceptance, before technical editing, formatting and proof reading. Using this free service, authors can make their results available to the community, in citable form, before we publish the edited article. This *Accepted Manuscript* will be replaced by the edited, formatted and paginated article as soon as this is available.

You can find more information about *Accepted Manuscripts* in the [Information for Authors](#).

Please note that technical editing may introduce minor changes to the text and/or graphics, which may alter content. The journal's standard [Terms & Conditions](#) and the [Ethical guidelines](#) still apply. In no event shall the Royal Society of Chemistry be held responsible for any errors or omissions in this *Accepted Manuscript* or any consequences arising from the use of any information it contains.

# Waterproof and breathable membranes of waterborne fluorinated polyurethane modified electrospun polyacrylonitrile fibers†

Cite this: DOI: 10.1039/x0xx00000x

Jiaqi Wang,<sup>†ab</sup> Yang Li,<sup>†ab</sup> Haiyang Tian,<sup>ab</sup> Junlu Sheng,<sup>bc</sup> Jianyong Yu,<sup>b</sup>  
Bin Ding<sup>\*abc</sup>

Received 00th January 2012,  
Accepted 00th January 2012

DOI: 10.1039/x0xx00000x

[www.rsc.org/](http://www.rsc.org/)

Creating an efficient and cost-effective approach that can provide advanced microporous membranes with high waterproofness and good breathability has proved to be an tremendous challenging. This work responds to these challenges by designing, fabricating and evaluating an electrospun polyacrylonitrile (PAN) fibrous membrane which were modified with waterborne fluorinated polyurethane (WFPU) to achieve high waterproof and breathable performances. By employing the WFPU modification, the pristine PAN fibrous membranes possessed remarkable superhydrophobicity with an advancing water contact angle of 159° as well as adjustable pore structure. Significantly, the waterproofness had confirmed to be depending on the maximum pore size and surface wettability finely accordance with the Young-Laplace equation, and a geometric coefficient A was introduced as a geometric factor to evaluate the torturous pore structure in electrospun fibrous membranes. Furthermore, the resultant membranes could present a high waterproofness to 83.4 kPa, large water vapor transmission rate over 9.2 kg/m<sup>2</sup>/d, good air permeability over 5.9 L/m<sup>2</sup>/s, suggesting the promising candidates for a variety of potential applications such as protective clothing.

## Introduction

Waterproof and breathable microporous membranes with performances like 'biomimetic skin' have attracted tremendous attention, owing to their characteristics to block water penetration and permit vapor transmission, as well as array of potential applications such as protective clothing, membrane distillation, pharmaceutical industry, and tissue engineering.<sup>1-4</sup> Generally, these membranes are fabricated from hydrophobic raw materials and exhibit a clearly visible system of pores as interconnected passage-ways, which enable small size gases and vapor to permeate through, but prevent liquid water from wetting and penetration.<sup>5, 6</sup> Ideally, demands not only for the pore size should be small enough to withstand penetration of liquid water, but also for the porosity should be as high as possible to maximize the vapor transmission.

Currently, a variety of strategies have been developed to fabricate waterproof and breathable microporous membranes, including mechanical fibrillation,<sup>7</sup> phase separation,<sup>8</sup> template methods,<sup>9</sup> and melt blown.<sup>10</sup> Unfortunately, these methods suffer from the complicated procedures or high cost, and in the meantime, the difficulties in regulating pore size and porosity make the fabricated membranes unable to satisfy the requirement in waterproof and breathable application.

Electrospinning has been proved to be an efficient method to fabricate microporous membranes with interconnected and controllable porous structure constructed by fibers accumulating, which could be facilely regulated by tuning fiber diameter and packing density.<sup>11, 12</sup> Up to now, electrospun microporous membranes with waterproof and breathable performances have been prepared, including polyurethane,<sup>13</sup> polypropylene,<sup>14</sup> and polyamide.<sup>15</sup> Also reported is that the preparation of electrospun polyurethane microporous membranes containing low surface energy content, which resulted in enhanced water resistance with a hydrostatic pressure of 39 kPa, and elevated breathability with a water vapor transmission (WVT) rate of 9 kg/m<sup>2</sup>/d.<sup>16</sup> However, the membranes still could not satisfy the demand of waterproof and breathable performances due to their relatively large pore size and low porosity, and the poor mechanical properties remain a limitation in the practical application.

To achieve electrospun microporous membranes with excellent waterproof and breathable performances and high tensile strength, the fabrication of composite fibrous membranes by modified with desirable materials is urgently needed. Waterborne fluorinated polyurethane (WFPU) as a class of low surface energy and environmental friendly material for fabrics finishing, could induce a variety of desirable properties to the substrates such as hydrophobicity, adjustable

pore structure and reinforced mechanical properties, contributing to good waterproof and breathable performances.<sup>17, 18</sup> To date, scarcely effort has been devoted to the development of WFPU modified electrospun fibrous membranes with waterproof and breathable performances.

In this study, we demonstrate a fabrication of waterproof and breathable PAN fibrous membranes by modified with WFPU emulsion on electrospun PAN fibers. The wettability, pore size and adhesion structure of the membranes were finely controlled by tuning PAN and WFPU concentrations. Moreover, on the basis of the above characters, the waterproof, breathable and mechanical performances were thoroughly investigated. Significantly, Young-Laplace equation was used to evaluate the waterproofness depending on the maximum pore size and surface wettability with the introduction of a geometric coefficient. Eventually, PAN fibrous membranes modified with WFPU exhibiting superhydrophobic surface, minimum pore size and optimized adhesion structure was fabricated, which exhibited excellent waterproof, breathable and mechanical performances.

## Experimental

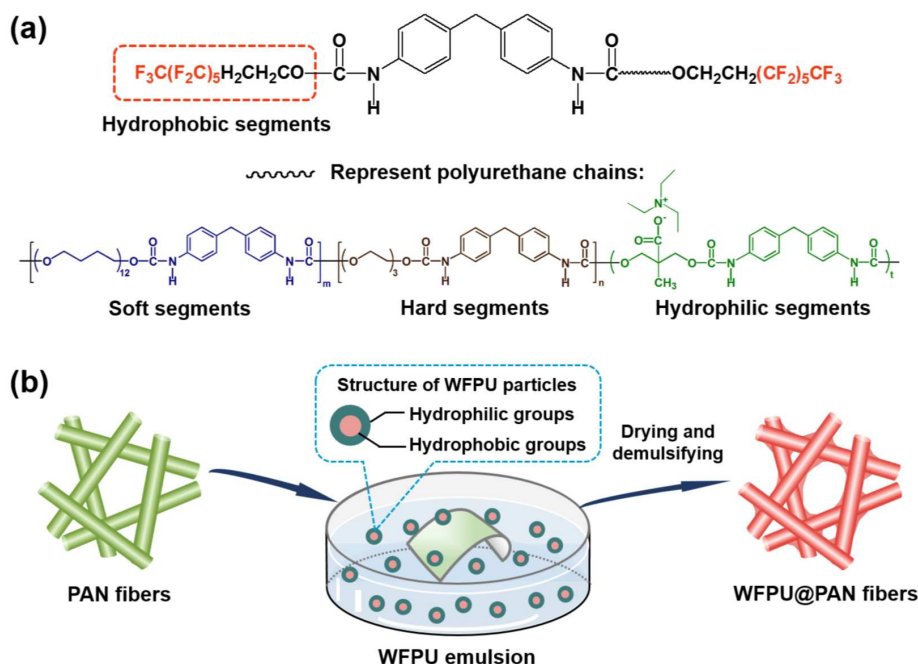
### Materials

Polyacrylonitrile (PAN,  $M_w = 90\ 000$  g/mol) was purchased from Kaneka Co., Ltd., Japan. 2-(Perfluorohexyl) ethyl alcohol (TEOH-6) was bought from Fuxin Heng Tong Fluorine Chemicals Co., Ltd., China. 4,4'-diphenylmethane diisocyanate

(MDI), triethylene glycol (TEG), polytetramethylene ether glycol (PTMEG,  $M_n = 1000$  g/mol), triethylamine (TEA), and 2,2'-dimethylol propionic acid (DMPA) was provided by Aladdin Chemical Co., China. *N,N*-dimethylformamide (DMF) and anhydrous calcium chloride were supplied by Shanghai Lingfeng Chemical Reagents Co., Ltd., China. Deionized water with a resistance of 18.2 M $\Omega$  was obtained from a Millipore system. All chemicals were used as received without further purification.

### Synthesis of waterborne fluorinated polyurethane

The WFPU was synthesized by accomplishing a self-emulsifying polymerization reaction. Typically, a mixture of MDI (20 g) and DMF (26 g) was added into a flask containing 17 g PTMEG and heated to 60 °C. After 1 h, TEG (2.55 g) was added to the above solution to give a chain extending reaction for 30 min. Subsequently, DMPA (4.35 g) as a hydrophilic group was poured into the flask and stirred for 15 min, then the mixture was heated to 75 °C, followed by the addition of 9.8 g TEOH-6 to obtain terminal fluorinated polyurethane chains. After a 1 h reaction period, TEA (3.28g) was added for the neutralization of carboxyl group in DMPA to obtain solubility in water and the mixture was cooled to the ambient temperature. Finally, 161 g deionized water was poured slowly into the flask and stirred vigorously for 2 h, and a WFPU emulsion with solid content of 25 wt% was obtained.



**Scheme 1** Schematic illustration of (a) chemical structure of WFPU particles and (b) the strategy for fabrication of WFPU@PAN fibrous membranes.

The chemical structure of WFPU was presented in Scheme 1a, and the detail procedures for preparing of WFPU emulsion were shown in the ESI (Fig. S1). The polymeric backbone of the WFPU was designed composing of soft, hard, hydrophilic and hydrophobic segments. The matrix of soft segments (PTMEG groups) and hard segments (urethane segments based on the MDI and TEG groups) would exhibit microphase separation and result in the superior mechanical properties. The carboxyl groups on DMPA was introduced as hydrophilic segments to disperse the polymer in aqueous medium. The low surface energy perfluoroalkane segments was situated on the head of the chain could facilely migrate to the surface region that would endow the polymer with promising hydrophobicity.

The structure confirmation by  $^1\text{H}$  and  $^{19}\text{F}$  nuclear magnetic resonance (NMR) spectroscopy and group affirmations by Fourier transform infrared (FT-IR) spectroscopy were also showed in the ESI (Fig. S2, S3, and S4). The particle size of the WFPU emulsion was determined by a particle size & zeta potential analyzer (Nano ZS, Malvern Instruments Ltd., UK). The distribution curve of particle size was showed in Fig. S5 revealing an average diameter of 26.6 nm. The molecular weight was characterized by the gel permeation chromatography method (GPC, PL-GPC 50, Polymer Laboratories Ltd., UK). The GPC curve of the WFPU was presented in Fig. S6 indicating that the molecular weight ( $M_w$ ) is 31120 and the polydispersity was 1.43.

### Preparation of PAN fibrous membranes

PAN solutions with concentrations of 6, 8, 10, 12, and 14 wt% were prepared by dissolving PAN into DMF with continuously stirring for 24 h at ambient temperature. The electrospinning process was carried out by using the DXES-1 spinning equipment (Shanghai Oriental Flying Nanotechnology Co., Ltd., China) with an applied high voltage of 25 kV, a feed rate of  $1 \text{ mL h}^{-1}$ , and a distance of 20 cm. Then, the electrospun PAN membranes were dried in vacuum oven to remove the residual solvent. The electrospinning chamber was kept with a constant temperature of  $24 \text{ }^\circ\text{C}$  and relative humidity of 45 %. All the membranes were fabricated with a thickness of  $30 \pm 2 \text{ }\mu\text{m}$ . The obtained PAN fibrous membranes fabricated from the PAN concentrations of  $x \%$  were denoted as PAN- $x$ .

### Fabrication of WFPU modified PAN fibrous membranes

WFPU emulsions with various concentrations of 1, 3, 5, 7, and 9 wt%, were prepared by mixing the synthesized WFPU emulsion with deionized water. A typical schematic illustration of the strategy for fabrication of WFPU modified PAN fibrous membranes was presented in Scheme 1b. The as-spun PAN fibrous membranes were immersed into the WFPU emulsions for 5 min, then, dried and demulsified in a vacuum oven for 10 min at  $70 \text{ }^\circ\text{C}$ . The corresponding WFPU modified PAN membranes were denoted as WFPU- $y$ @PAN- $x$  where  $y$  is the concentration ( $y \text{ wt}\%$ ) of WFPU emulsion, e.g., WFPU-

1@PAN-8 represented the 8 wt% PAN membrane modified with 1 wt% WFPU emulsion.

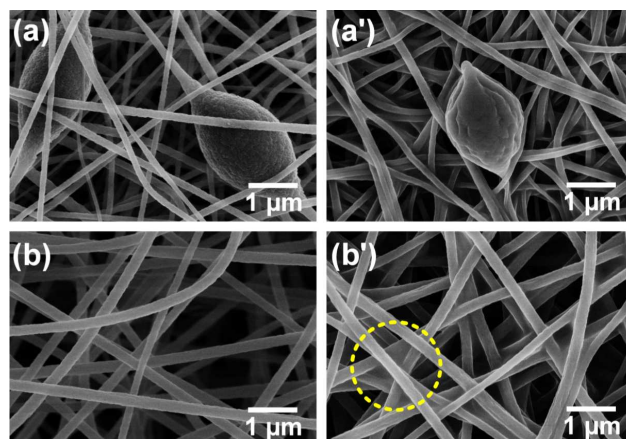


Fig. 1 FE-SEM images of (a) PAN-6, (a') WFPU-5@PAN-6, (b) PAN-8, and (b') WFPU-5@PAN-8 fibrous membranes.

### Characterization of the membranes

The morphology of the fibrous membranes were observed by a field emission scanning electron microscopy (FE-SEM, S-4800, Hitachi Ltd., Japan). Advancing contact angle of water ( $\theta_{adv}$ ) was measured by a contact angle goniometer Kino SL200B using the increment method. The mechanical properties of the membranes were tested on a tensile tester (XQ-1C, Shanghai New Fiber Instrument Co., Ltd., China). The thickness was measured by a thickness gauge (CHY-C2, Labthink Instruments Co., Ltd., China). The pore size and pore diameter distribution were characterized via the bubble point method by a capillary flow porometer (CFP-1100AI, Porous Materials Inc., USA).

### Measurements of waterproof and breathable performances

The hydrostatic pressure of the membranes were examined according to AATCC 127 standard test method by using a hydrostatic pressure tester (YG812C, Nantong Hongda Experiment Instruments Co., Ltd., China), with a water pressure increasing rate of  $6 \text{ kPa min}^{-1}$ . The WVT rate was evaluated according to ASTM E96-CaCl<sub>2</sub> standards desiccant method by using a water vapor transmission tester (YG 601H, Ningbo textile Instruments Co., Ltd., China), with constant temperature of  $38 \text{ }^\circ\text{C}$  and relative humidity of 90 %. The air permeability was measured according to ISO 9237:1995 standard test method by using a Frazier aid permeability tester (YG461E, Ningbo textile Instruments Co., Ltd., China), with a pressure drop of 100 Pa. The water absorption rate was examined according to AATCC 21-1993 standard, which characterized the percentage of weight increment of the samples after immersing in water for 20 min.

### Ethical statement

Fish was used in this manuscript to display the waterproof and breathable properties without any in vivo experiment. And the animal welfare was carried out in accordance with the guideline

for the Care and Use of Laboratory Animals and were approved by the animal ethics committee of Donghua University.

strong hydrogen bond between the cyano group (C≡N) in PAN and imino group(=NH) in

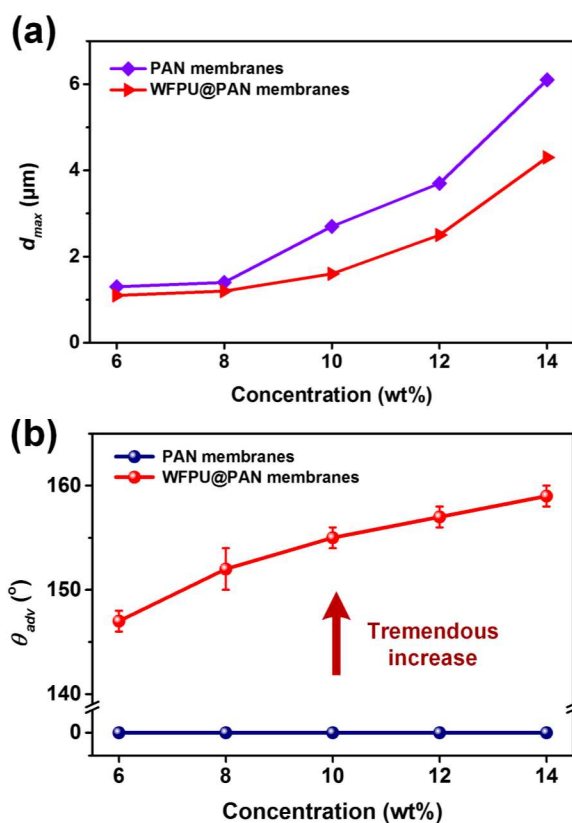


Fig. 2 (a)  $d_{max}$  and (b)  $\theta_{adv}$  of PAN and the corresponding WFPU-5@PAN fibrous membranes fabricated from various PAN concentrations.

## Results and discussion

The representative FE-SEM images of PAN fibers fabricated from various concentrations of PAN solutions are presented in Fig. 1 and Fig. S7, revealing that the fibers distributed randomly to form porous membranes. As shown in Fig. 1a, PAN-6 membranes exhibited a beads-on-string structures, which contain numerous submicro- and micro-sized elliptical beads along the individual fibers (average diameter is 158 nm). The formation of this structure could be attributed to the utilization of the PAN solution with low viscosity.<sup>19, 20</sup> However, with increasing the concentration of PAN solutions, the average fiber diameter increased from 209 to 737 nm, and the elliptical beads along the fiber axis disappeared as well. More interestingly, the morphology of the WFPU-5@PAN fibrous membranes were greatly changed comparing with the pristine ones, as shown in Fig. 1a'-b' and Fig. S7a'-c'. The average fiber diameter of WFPU-5@PAN fibrous membranes formed from 6, 8, 10, 12, and 14 wt% PAN concentrations were 190, 256, 365, 529, and 788 nm, respectively. It indicates that the fibers diameter would be increased obviously after covered by WFPU with thickness of 15-25 nm, which is due to the

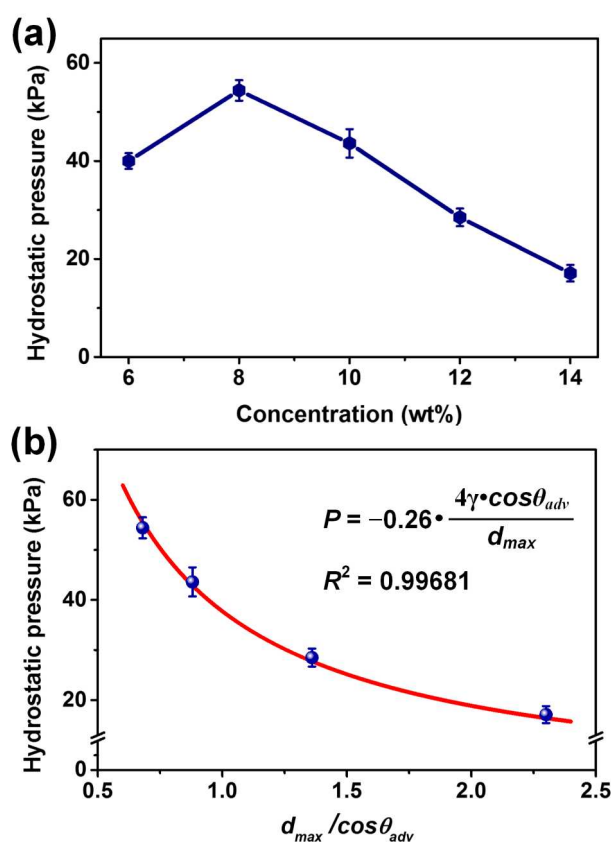


Fig. 3 (a) Hydrostatic pressure, and (b) dependence of hydrostatic pressure on  $d_{max}$  and  $\theta_{adv}$  of WFPU-5@PAN fibrous membranes fabricated from various PAN concentrations.

WFPU.<sup>21, 22</sup> In addition, numerous adhesion structure among the adjacent fibers was observed, which was formed by WFPU emulsions. During the modification, WFPU emulsions filled the voids and formed bonding (yellow circle in Fig. 1b').

Intended to investigate the effect of WFPU modification on the porous structure, pore size distribution was measured through capillary flow porometer (Fig. 2b). The maximum pore size ( $d_{max}$ ) of the PAN fibrous membranes increased remarkably from 1.3 to 6.1  $\mu\text{m}$ , which is due to the increase of fiber diameter.<sup>23, 24</sup> Moreover, after modified with WFPU emulsion, the  $d_{max}$  of WFPU-5@PAN fibrous membranes fabricated from various PAN concentrations were 1.1, 1.2, 1.6, 2.5, and 4.3  $\mu\text{m}$ , respectively. Comparing with the corresponding unmodified PAN membranes, all the samples exhibit a significant reduction in  $d_{max}$ , which is due to the formation of the adhesion structure among adjacent fibers that filled the voids.<sup>25</sup>

On the other hand, the wetting behavior of both PAN and WFPU-5@PAN fibrous membranes was evaluated by measuring the  $\theta_{adv}$  of water on the membranes, as shown in Fig. 2b. The PAN fibrous membranes showed superhydrophilicity

due to the presence of polar cyano group in the skeletal chain.<sup>20, 26</sup> After

of  $d_{max}$  (Fig. 2a). Moreover, the hydrostatic pressure of porous membranes could be determined using the Young-Laplace equation, which is commonly used to express the liquid enter pressure of a cylindrical capillary:

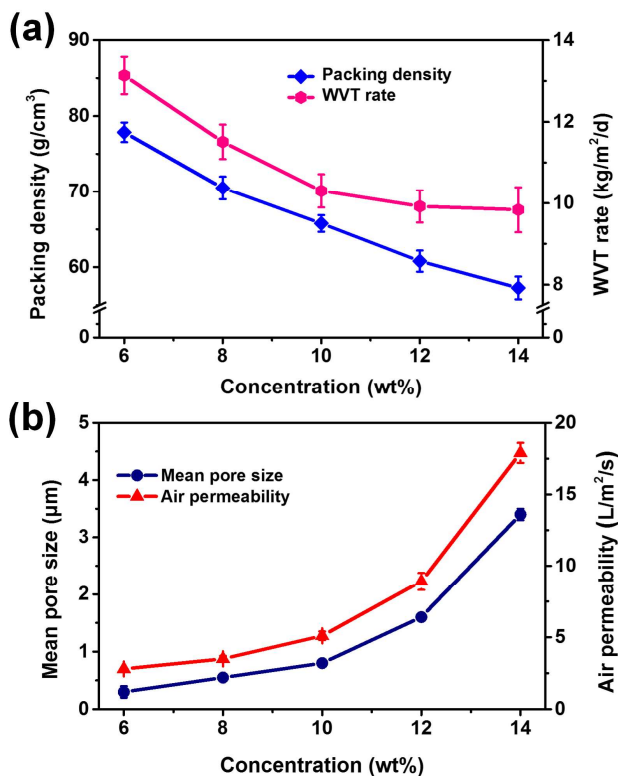


Fig. 4 (a) Porosity and WVT rate, and (b) mean pore size and air permeability of WFPU-5@PAN fibrous membranes fabricated from various PAN concentrations.

WFPU modification, a tremendous transition in wetting behavior has been observed here, the  $\theta_{adv}$  which increases from 0 to higher than 140°, which is due to the high fraction of coverage on the PAN fibers by WFPU with low surface energy fluorinated segment.<sup>16, 27</sup> Furthermore, the  $\theta_{adv}$  of the WFPU@PAN membranes increased from 147 to 159° with PAN concentrations increasing from 6 to 14 wt%, which is attributed to the increased roughness by larger fiber diameter.<sup>28, 29</sup>

As expected, the  $d_{max}$  and wettability would highly influence the waterproofness through a synergetic effect. The waterproofness of the WFPU-5@PAN fibrous membranes was investigated by evaluating the hydrostatic pressure (Fig. 3a). An increase of hydrostatic pressure from 40 to 54.4 kPa was observed when the PAN concentration increased from 6 to 8 wt%, owing to the disappearance of bead-on-string structure, which lead to enhanced tensile strength and reduced deformation of the pores under external water pressure. However, with further increasing of PAN concentrations to 14 wt%, an obvious decrease of hydrostatic pressure from 44.9 to 16.1 kPa was emerged, which is due to the remarkable increase

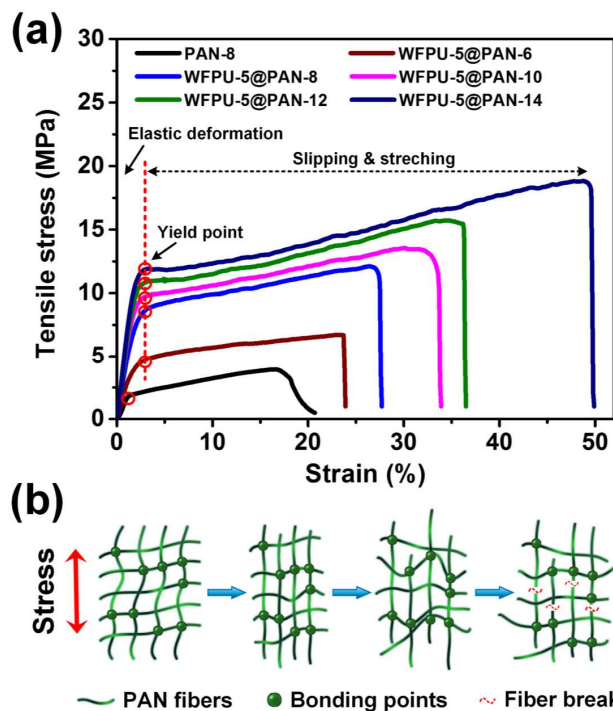


Fig. 5 (a) Stress-strain curves of PAN-8 and WFPU-5@PAN fibrous membranes. (b) Proposed break mechanism of tensile fracture process upon external stress.

$$P = -\frac{4A \cdot \gamma \cos \theta_{adv}}{d_{max}} \quad (1)$$

where  $P$  is the hydrostatic pressure,  $\gamma$  is the surface tension of water, and  $d_{max}$  is the maximum pore diameter, as that is the most vulnerable to be wetted by water.<sup>30, 31</sup> In this equation, the coefficient  $A$  is introduced as a geometric factor to assume the non-cylindrical pore as 'equivalent cylindrical pore', which is related to the torturous pore structure constructed by the accumulating of fibers. Significantly, the hydrostatic pressure has confirmed to depend on the  $d_{max}$  and  $\theta_{adv}$  finely accordance with the Young-Laplace equation, and presented a coefficient  $A$  of 0.26 (Fig. 3b).

On the basis of the excellent waterproofness, the breathable performance of WFPU-5@PAN fibrous membranes was studied by measuring WVT rate and air permeability (Fig. 4). WVT rate would be highly influenced by porosity of the membranes. As shown in Fig. 4a, the porosity decrease from 77.8 to 57.3% towards increasing of PAN concentrations, which result in a decrease of WVT rate from 13.1 to 9.8 kg/m<sup>2</sup>/d. This is attributed to that more WFPU emulsion would be adsorbed in the membranes with larger pore size resulting in more adhesion structure formation. Moreover, since the air permeability was measured under a pressure drop of 100 Pa, the

mean pore size was the foremost parameter that affect the air permeability.<sup>32, 33</sup>

5@PAN membranes with numerous bonding structure resulted from the break of fibers between bonding points, thus displayed enhanced tensile strength and elongation. The tensile strength of WFPU-5@PAN

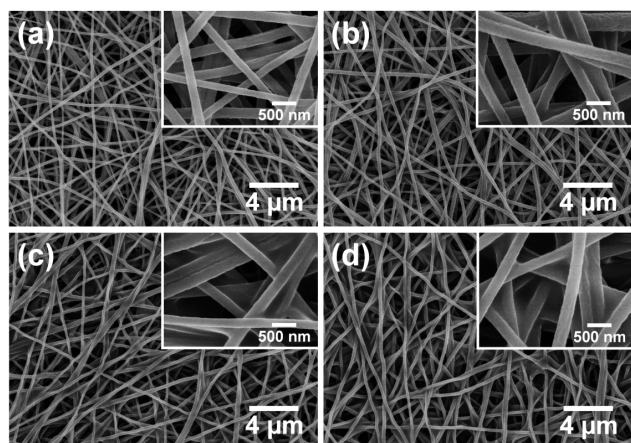


Fig. 6 FE-SEM images of (a) WFPU-1@PAN-8, (b) WFPU-3@PAN-8, (c) WFPU-7@PAN-8, and (d) WFPU-9@PAN-8 fibrous membranes.

Therefore, a remarkable increase in air permeability from 2.8 to 17.9 L/m<sup>2</sup>/s was observed with the increasing of PAN concentrations, which is attributed to the increase of mean pore size (Fig. 4b).

Mechanical property is another important factor in practical application, which could be tremendously enhanced during the WFPU modifying process. Generally, the mechanical behaviors of electrospun fibrous membranes are closely related to the geometric arrangement and the bonding structure among the fibers.<sup>34, 35</sup> As shown in Fig. 1 and Fig. S7, the PAN and WFPU-5@PAN fibrous membranes exhibited randomly oriented geometry, thus the bonding structure becomes the key factor that affect the mechanical behaviors. Typical tensile stress-strain curves of PAN-8 and WFPU-5@PAN fibrous membranes (Fig. 5a). It is clearly observed that all the membranes exhibited a linear elastic deformation in the first region under a stress load before reaching the yield point, then, the stress-strain curves showed a nonlinear increase with the continuous loaded stress until break.

This mechanical behavior could be explained by the two-step break mechanism, as illustrated in Fig. 5b.<sup>36, 37</sup> When a small external stress was loaded, the randomly oriented fibers tend to align along the strain direction, and the fibers between bonding points would undertake the stress on intermolecular level, resulting in the liner deformation with an elongation less than 3%. After reaching the yield points, the curves showed a nonlinear elasticity which is related to the slipping and stretching of individual fiber along stress direction. Finally, the PAN-8 fibrous membranes broke due to the non-bonding fibers slipped apart, which exhibited a nonlinear decrease with the minimum tensile strength (3.7 MPa) and elongation (21.2 %) at break. All the PAN fibrous membranes exhibited similar mechanical properties (Fig. S8). However, the break of WFPU-

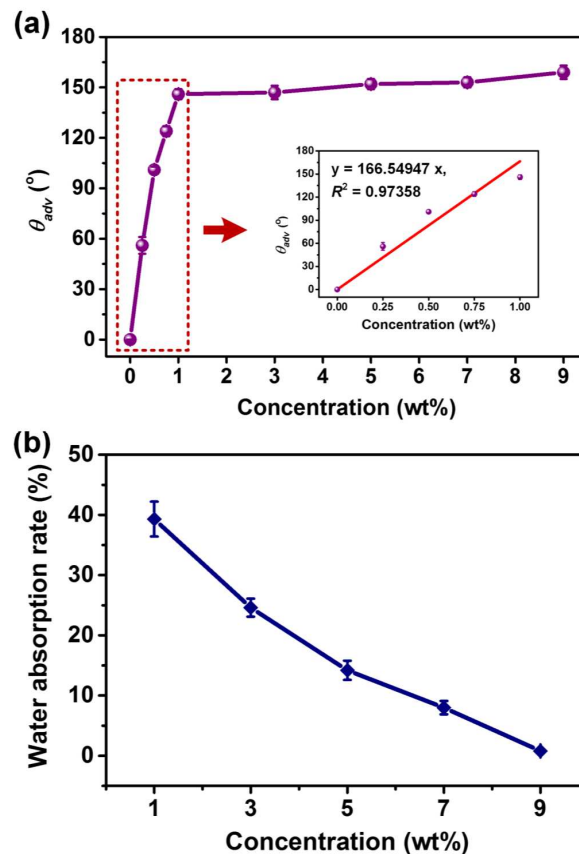


Fig 7 (a)  $\theta_{adv}$ , and (b) water absorption rate of WFPU@PAN-8 fibrous membranes modified with WFPU emulsions of various concentrations.

fibrous membranes formed from 6, 8, 10, 12, and 14 wt% PAN solutions were 8.5, 12.1, 13.5, 16.7, and 18.8 MPa, respectively, indicating that the tensile strength increases with the disappearance of the beads and the increase of fiber diameter.<sup>38, 39</sup> Considering the practical application, the membranes should not only possess good mechanical properties, but also exhibit high waterproofness and breathability PAN-8 fibrous membranes was carried out in the following study.

In order to explore the real waterproofness and breathability of WFPU@PAN fibrous membranes, the PAN-8 fibrous membranes modified with various concentrations of WFPU emulsions were investigated. The representative FE-SEM images of WFPU@PAN-8 fibrous membranes modified with various WFPU concentrations are presented in Fig. 6, revealing that more adhesion structure was formed between the voids of fibers with increasing of the WFPU concentrations. Besides that, the pore size distribution of the membranes showed in the

range of 0.2 to 1.3  $\mu\text{m}$ , and the mean pore size decreased gradually with the increasing of WFPU concentrations, which is due to more adhesion structure formed among fibers (Fig. S9).

Since the WFPU@PAN fibrous membranes were influenced by two opposite characteristics, including the hydrophilicity of PAN and the hydrophobicity of WFPU emulsion, the wettability

was studied by estimating  $\theta_{adv}$  and water absorption rate. As can be seen in Fig. 7a, only using low WFPU concentration (1 wt%) would obtain a tremendous increase in  $\theta_{adv}$  from 0 to  $146^\circ$ , confirming that a critical concentration of WFPU could induce the hydrophobicity among the hydrophilic PAN fibrous membranes. Moreover, the use of 0.25, 0.5, 0.75, and 1 wt% WFPU resulted in a liner increase in  $\theta_{adv}$  of 56, 101, 124, and  $146^\circ$  (inset of Fig. 7a). Additionally, further increase of WFPU concentrations to 9 wt% have revealed a continued increase in  $\theta_{adv}$  to  $159^\circ$ , owing to more fluorinated segments enriched on the surface of fibers. On the other hand, the water absorption rate decrease gradually from 40 to 0.8% with the WFPU concentrations increasing from 1 to 9 wt%, indicating that membranes modified with higher WFPU concentration would exhibit much better hydrophobicity, as shown in Fig. 7b. The increase in  $\theta_{adv}$  and the decrease in water absorption rate would contributed to higher waterproof and breathable performances.

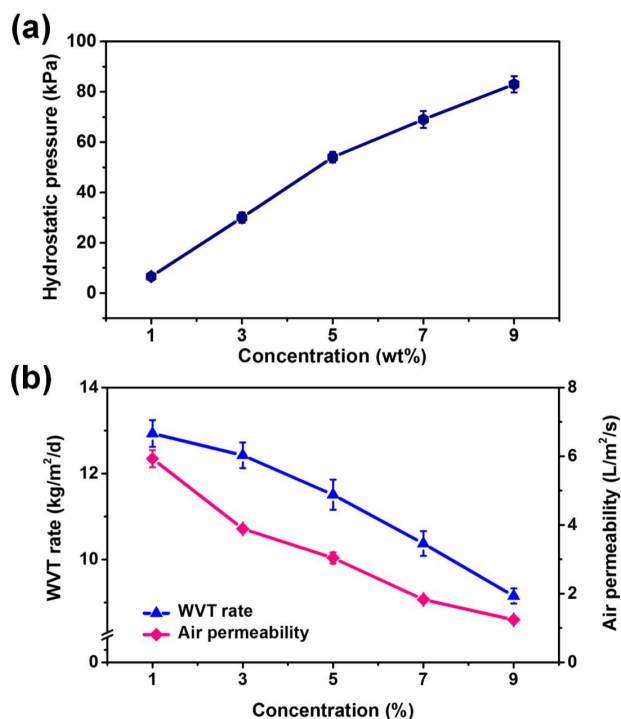
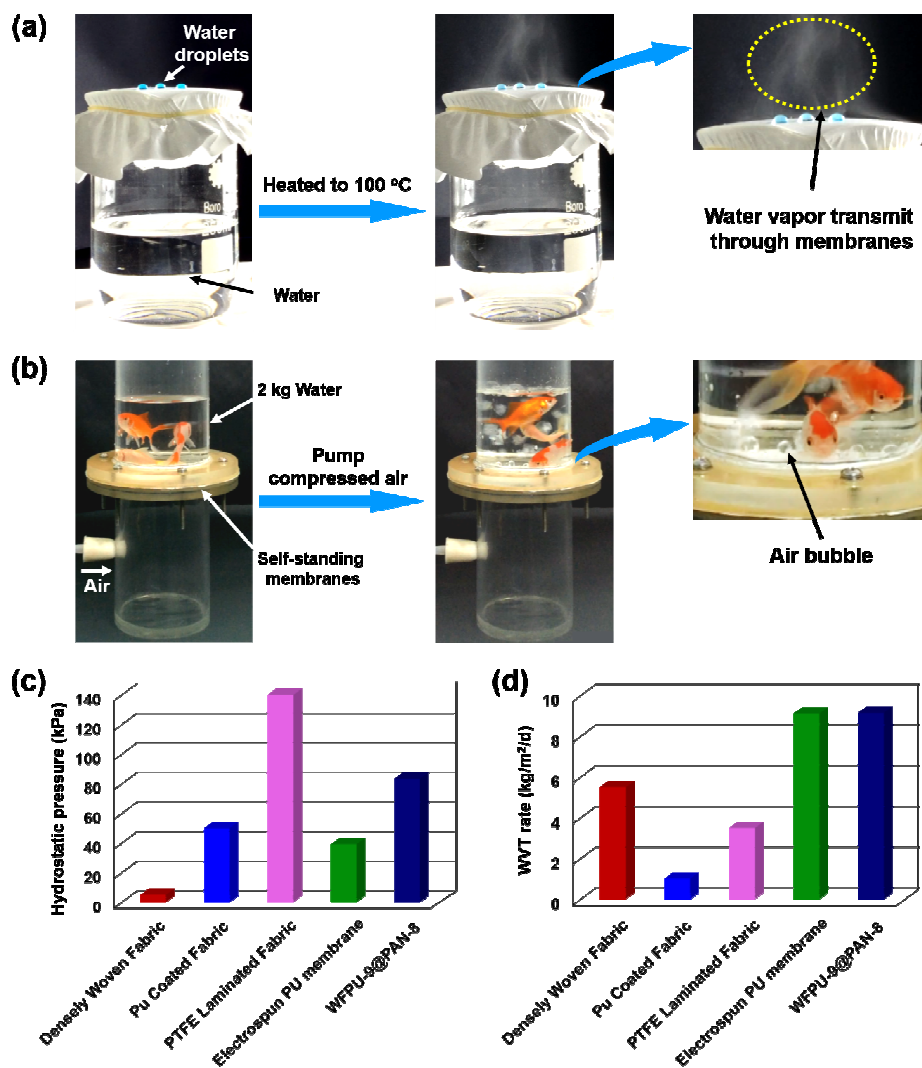


Fig. 8 (a) Hydrostatic pressure and (b) WVT rate and air permeability of WFPU@PAN fibrous membranes modified with various concentrations of WFPU emulsions

The effect of WFPU emulsion modification on the performances of the WFPU@PAN-8 fibrous membranes was confirmed by measuring hydrostatic pressure, WVT rate, air permeability, and mechanical properties, as shown in Fig. 8. The hydrostatic pressure increased from 6.6 to 83.4 kPa, revealing that the waterproof properties increased regularly towards increasing of WFPU concentrations, which is due to the increase of  $\theta_{adv}$  and the decrease of the water absorption rate. However, the WVT rate decreased from 12.9 to 9.2 kg/m<sup>2</sup>/d, which is due to the increased adhesion structure that filled more voids between fibers. Nevertheless, with the decreasing of mean pore size, the air permeability decrease from 5.9 to 1.2 L/m<sup>2</sup>/s. Furthermore, the tensile strength increased from 7.1 to 14.4 MPa with the increasing of WFPU concentrations, which is due to more formation of adhesion structure, as shown in Fig. S10. These results illustrated that the hydrostatic pressure, WVT rate and air permeability could be regulated simultaneously by diversifying WFPU concentrations, which provide a facile and efficient method to produce membranes with various waterproofness and breathability.

Above all, the WFPU@PAN fibrous membranes which combined hydrophobicity, diminutive pore sizes and good mechanical properties, demonstrated excellent water resistance and breathability. Two typical tests in Fig. 9 were performed as proofs of waterproof and breathable performances of WFPU-9@PAN-8 fibrous membrane. As shown in Fig. 9a, the WFPU-9@PAN-8 membrane was covered on a beaker with water, and three droplets of colored water were dripped upon the membrane. Abundant vapor was produced after heating the water to 100 °C, and facilely transmitted through the membrane, indicating an outstanding transmission rate of water vapour (Movie S1†). Moreover, a severe but interesting test was performed as a further confirmation of the waterproof and breathable performances, as shown in Fig. 9b. The self-standing WFPU-9@PAN-8 fibrous membrane were fixed between a close chamber (with an air inlet pipe, left panel of Fig. 9b) and an open tube, and 2 kg water were larded upon the membrane. The membrane could afford the weight of water without penetration, while air could transmit through by pump compressing (middle panel in Fig. 9b). Close observation (right panel in Fig. 9b) showed that the air bubbles that formed from the permeated air were generated on the surface of the membrane, revealing an extremely high air permeability (Movie S2†). Additionally, a comparison with performance of the conventional waterproof and breathable art systems was presented in Fig. 9c and d, indicating that the WFPU-9@PAN-8 membranes exhibited high hydrostatic pressure and WVT rate. Consequently, the WFPU@PAN fibrous membrane exhibited excellent waterproof and breathable performances, suggesting a promising candidate for a variety of potential applications in protective clothing, membrane distillation, pharmaceutical industry, tissue engineering and filtration/separation process, etc.





**Fig. 9** Two typical tests demonstrating the waterproof and breathable performances of WFPU-9@PAN-8 fibrous membrane. (a) Three droplets of colored water were dripped on the surface of the membrane, while abundant water vapor could facilitate transmit through the membrane. (b) 2 kg of water could load on the self-standing membrane without water leakage, but air bubbles could transmit through the membrane by pump compressing at the same time. (c) Hydrostatic pressure and (d) WVT rate of WFPU-9@PAN-8 fibrous membrane and conventional waterproof and breathable fabrics.

## Conclusions

In summary, we have described the preparation of electrospun PAN fibrous membrane exhibiting excellent waterproof and breathable performances by modification with a novel synthesized WFPU emulsion. The introduction of the low surface energy segments in WFPU enabled the resultant membranes to show superhydrophobicity ( $159^\circ$ ). The WFPU@PAN fibrous membranes with numerous adhesion structure showed adjustable pore structure and relatively high tensile strength (14.4 MPa) by varying the PAN and WFPU concentrations. Significantly, the hydrostatic pressure has confirmed to depend on the  $d_{max}$  and  $\theta_{adv}$  finely accordance with the Young-Laplace equation. Moreover, the dependence of hydrostatic pressure on  $d_{max}$  and  $\theta_{adv}$  was confirmed to be finely accordance with the Young-Laplace equation. Significantly, the as-prepared membranes exhibited excellent waterproofness of 83.4 kPa, good water vapor transmission rate of 9.2 kg/m<sup>2</sup>/d and air permeability of 5.9 L/m<sup>2</sup>/s, suggesting as a promising

candidate for a variety of potential applications, such as protective clothing, membrane distillation, pharmaceutical industry, tissue engineering, and water filtration.

## Acknowledgements

This work is supported by the National Natural Science Foundation of China (No. U1232116 and 51322304), the Program for New Century Talents of the University in China, the Fundamental Research Funds for the Central Universities, and the “DHU Distinguished Young Professor Program”.

## Notes and references

- <sup>a</sup> State Key Laboratory for Modification of Chemical Fibers and Polymer Materials, College of Material Science and Engineering, Donghua University, Shanghai 201620, China. E-mail: binding@dhu.edu.cn  
<sup>b</sup> Nanomaterials Research Center, Modern Textile Institute, Donghua University, Shanghai 200051, China

<sup>©</sup> Key Laboratory of Textile Science & Technology, Ministry of Education, College of Textiles, Donghua University, Shanghai 201620, China

<sup>†</sup> Electronic Supplementary Information (ESI) available: Details synthesis and structure confirmation of WFPU, FE-SEM, stress-strain curves of PAN and WFPU@PAN-8 membranes, pore size distribution and maximum pore size of WFPU@PAN-8 membranes, and Movies S1 and S2. See DOI: 10.1039/b000000x/

<sup>‡</sup> These authors have contributed equally to this work.

- 1 A. H. Wook, P. C. Hee and C. S. Eun, *Text. Res. J.*, 2011, **81**, 1438-1447.
- 2 X. Wang, B. Ding, J. Yu and M. Wang, *Nano Today*, 2011, **6**, 510-530.
- 3 B. S. Lalia, E. G. Burrieza, H. A. Arafat and R. Hashaikeh, *J. Membr. Sci.*, 2013, **428**, 104-115.
- 4 X. Wang, B. Ding and B. Li, *Mater. Today*, 2013, **16**, 229-241.
- 5 P. W. Gibson, *Polym. Test.*, 2000, **19**, 673-691.
- 6 A. Gugliuzza and E. Drioli, *J. Membr. Sci.*, 2013, **446**, 350-375.
- 7 S. H. Tabatabaei, P. J. Carreau and A. Ajji, *J. Membr. Sci.*, 2008, **325**, 772-782.
- 8 Y. Li, G. He, S. Wang, S. Yu, F. Pan, H. Wu and Z. Jiang, *J. Mater. Chem. A*, 2013, **1**, 10058-10077.
- 9 J. H. Pan, H. Dou, Z. Xiong, C. Xu, J. Ma and X. S. Zhao, *J. Mater. Chem.*, 2010, **20**, 4512-4528.
- 10 B. Yu, J. Han, X. He, G. Xu and X. Ding, *J. Macromol. Sci. B*, 2012, **51**, 619-629.
- 11 X. Wang, B. Ding, G. Sun, M. Wang and J. Yu, *Prog. Mater. Sci.*, 2013, **58**, 1173-1243.
- 12 C. Erisken, D. M. Kalyon and H. Wang, *Biomaterials*, 2008, **29**, 4065-4073.
- 13 J. Hu, X. Wang, B. Ding, J. Lin, J. Yu and G. Sun, *Macromol. Rapid Commun.*, 2011, **32**, 1729-1734.
- 14 D. W. Huttmacher and P. D. Dalton, *Chemistry-an Asian Journal*, 2011, **6**, 44-56.
- 15 S. Sinha-Ray, M. W. Lee, S. Sinha-Ray, S. An, B. Pourdeyhimi, S. S. Yoon and A. L. Yarin, *J. Mater. Chem. C*, 2013, **1**, 3491-3498.
- 16 J. Ge, Y. Si, F. Fu, J. Wang, J. Yang, L. Cui, B. Ding, J. Yu and G. Sun, *RSC Adv.*, 2013, **3**, 2248-2255.
- 17 W. C. Jiang, Y. Huang, G. T. Gu, W.-D. Meng and F.-L. Qing, *Appl. Surf. Sci.*, 2006, **253**, 2304-2309.
- 18 P. Krol, B. Krol, R. Stagraczynski and K. Skrzypiec, *J. Appl. Polym. Sci.*, 2013, **127**, 2508-2519.
- 19 H. Fong, I. Chun and D. H. Reneker, *Polymer*, 1999, **40**, 4585-4592.
- 20 T. Ren, Y. Si, J. Yang, B. Ding, X. Yang, F. Hong and J. Yu, *J. Mater. Chem.*, 2012, **22**, 15919-15927.
- 21 W. Pan, S. L. Yang, G. Li and J. Jiang, *Eur. Polym. J.*, 2005, **41**, 2127-2133.
- 22 Y. Liu, J. H. Xin and C.-H. Choi, *Langmuir*, 2012, **28**, 17426-17434.
- 23 W. Sambaer, M. Zatloukal and D. Kimmer, *Chem. Eng. Sci.*, 2011, **66**, 613-623.
- 24 N. Wang, Z. Zhu, J. Sheng, S. S. Al-Deyab, J. Yu and B. Ding, *J. Colloid Interf. Sci.*, 2014, **428**, 41-48.
- 25 N. Wang, Y. Si, N. Wang, G. Sun, M. El-Newehy, S. S. Al-Deyab and B. Ding, *Sep. Purif. Technol.*, 2014, **126**, 44-51.
- 26 K. H. Sung, *J. Polym. Sci., Part B (Polymer Physics)*, 1996, **34**, 1181-1187.
- 27 A. Raza, B. Ding, G. Zainab, M. El-Newehy, S. S. Al-Deyab and J. Yu, *J. Mater. Chem. A*, 2014, **2**, 10137-10145.
- 28 M. W. Lee, S. An, S. S. Latthe, C. Lee, S. Hong and S. S. Yoon, *ACS Appl. Mater. Inter.*, 2013, **5**, 10597-10604.
- 29 J. Wang, A. Raza, Y. Si, L. X. Cui, J. F. Ge, B. Ding and J. Y. Yu, *Nanoscale*, 2012, **4**, 7549-7556.
- 30 R. B. Saffarini, B. Mansoor, R. Thomas and H. A. Arafat, *J. Membr. Sci.*, 2013, **429**, 282-294.
- 31 Z. D. Hendren, J. Brant and M. R. Wiesner, *J. Membr. Sci.*, 2009, **331**, 1-10.
- 32 H. Wan, N. Wang, J. Yang, Y. Si, K. Chen, B. Ding, G. Sun, M. El-Newehy, S. S. Al-Deyab and J. Yu, *J. Colloid Interf. Sci.*, 2014, **417**, 18-26.
- 33 R. A. Abuzade, A. Zadhoush and A. A. Gharehaghaji, *J. Appl. Polym. Sci.*, 2012, **126**, 232-243.
- 34 K. Lee, B. Lee, C. Kim, H. Kim, K. Kim and C. Nah, *Macromol. Res.*, 2005, **13**, 441-445.
- 35 W.-I. Baek, H. R. Pant, R. Nirmala, K.-T. Nam, H.-J. Oh and H.-Y. Kim, *Polym. Int.*, 2012, **61**, 844-849.
- 36 J. Lin, B. Ding, J. Yang, J. Yu and S. S. Al-Deyab, *Mater. Lett.*, 2012, **69**, 82-85.
- 37 F. Zhao, X. Wang, B. Ding, J. Lin, J. Hu, Y. Si, J. Yu and G. Sun, *RSC Adv.*, 2011, **1**, 1482-1488.
- 38 X. Mao, Y. C. Chen, Y. Si, Y. Li, H. G. Wan, J. Y. Yu, G. Sun and B. Ding, *RSC Adv.*, 2013, **3**, 7562-7569.
- 39 N. Robertson, *Angew. Chem. Int. Edit.*, 2008, **47**, 1012-101433.